Master's Thesis

Adeno-associated viral vector injection reduces adult hippocampal neurogenesis in mouse brain

Veera Puumalainen

University of Jyväskylä

Department of Biological and Environmental Science

12 November 2023

UNIVERSITY OF JYVÄSKYLÄ, Faculty of Mathematics and Science
Department of Biological and Environmental Science
Master's Degree Programme in Cell and Molecular Biology

Puumalainen, Veera

Adeno-associated viral vector injection reduces adult hippocampal neurogenesis in mouse brain

MSc Thesis: 30 p.
Supervisors: Docent Sanna Lensu and Prof. Jari Ylänne
Reviewers: PhD Jonna Nykky and MSc Kimmo Lehtinen

November 2023

Keywords: adeno-associated virus, brain, calcium imaging, dentate gyrus, hippocampus, learning, memory, mouse, neurogenesis

During adulthood, new neurons are mainly generated in hippocampal dentate gyrus. This process is known as adult hippocampal neurogenesis (AHN), during which neural progenitor cells divide, and mature into adult-born dentate granule cells. Finally they integrate into hippocampal networks, which are known to take part in learning and memory. Calcium imaging methods have permitted studying the cellular level events of learning and memory *in vivo*. For this, genes encoding for fluorescent calcium indicators are conveyed to neuronal cells, and when coupled with micro-optical tools they enable the live monitoring of calcium activity, reflecting activation of neurons. Adeno-associated virus (AAV) is one of the most used genetic vectors for calcium indicator expression on the target cells. AAVs are regarded as safe and effective, and so recombinant AAVs are developed increasingly to deliver transgenes to target tissues. However, recent research has revealed AAVs' potency to induce cell death in many cell types, including neural progenitor cells and adult-born neurons. In this study, the AAV-induced effects on AHN were assessed by injecting saline (n=6) or AAV9 vector carrying GCaMP6s calcium indicator unilaterally to dentate gyri of adult male mice (n=10). After ca. 33 weeks, the number of adult-born neurons was determined bilaterally by doublecortin immunolabeling and confocal microscopy. In addition, the amount of GCaMP6s-derived green fluorescence (GF) was measured as a marker for transgene expression. Ipsilaterally to the injection, AAV reduced the number of adult-born neurons, i.e., neurogenesis, in comparison to saline-injected control group. The effect was local, since the number of new neurons in the contralateral hemisphere of AAV injected mice did not differ from control group. Surprisingly, no association between the GF intensity and the decrease of neurogenesis was found, and the reason for this lack of correlation remains unclear. In conclusion, this study shows the harmful effect of AAV on AHN and agrees with the scarce amount of existing data on this concern. This issue demands further research since AAVs are among the leading gene therapy vectors and research tools, also within central nervous system.

JYVÄSKYLÄN YLIOPISTO, Matemaattis-luonnontieteellinen tiedekunta
Bio- ja ympäristötieteiden laitos
Solu- ja molekyylibiologian maisteriohjelma

Puumalainen, Veera

Adeno-assosioitu virusvektori vähentää aikuisiän hermosolujen uusiutumista hiiren hippokampuksessa

Pro gradu -tutkielma: 30 s.
Työn ohjaajat: Dosentti Sanna Lensu ja Professori Jari Ylänne
Tarkastajat: FT Jonna Nykky ja FM Kimmo Lehtinen

Marraskuu 2023

Hakusanat: adeno-assosioitu virus, aivot, hiiri, hippokampus, kalsiumkuvantaminen, muisti, neurogeneesi, oppiminen, pykäläpoimu

Aikuisiällä uusia hermosoluja syntyy pääosin hippokampuksen pykäläpoimussa, jossa hermokantasolut jakautuvat ja kypsyvät toiminnallisiksi jyväissoluiksi, jotka liittyvät lopulta hippokampuksen hermoverkkoihin. Tämä ilmiö tunnetaan aikuisiän hippokampaalisena neurogeneesinä. Kalsiumkuvantaminen yhdistettynä mikro-optisiin työkaluihin mahdollistaa muistille ja oppimiselle tärkeiden hippokampuksen hermosolujen aktiivisuuden tutkimisen elävän eläimen aivoissa. Kuvantamisen mahdollistamiseksi kohdesolu täytyy saada ilmentämään fluoresoivaa kalsiumindikaattoria. Tätä varten soluun kuljetetaan vektorin avulla sitä koodaava geeni. Yksi käytetyimmistä vektoreista on yleisesti turvallisena pidetty adeno-assosioitu virus (AAV), ja useita siihen perustuvia tutkimusmenetelmiä ja geeniterapiamuotoja onkin kehitetty ja yhä kehitteillä. AAV:n on kuitenkin vastikään raportoitu aiheuttavan solukuolemaa useissa solutyypeissä, mukaan lukien hermokantasolut ja aikuisiällä syntyneet hermosolut. Tässä tutkielmassa AAV:n vaikutusta uusiin hermosoluihin tutkittiin aikuisilla uroshiirillä (n=10), joiden toisen aivopuoliskon pykäläpoimuihin injektoitiin GCaMP6s-kalsiumindikaattoria koodaavaa AAV9-vektoria. Noin 33 viikon kuluttua aivot siivutettiin, ja uudet hermosolut värjättiin kaksoiskortiini-vasta-aineella ja laskettiin molemmista aivopuoliskoista konfokaalimikroskoopilla. Lisäksi GCaMP6s:n tuottaman fluoresenssin määrä mitattiin hippokampuksista AAV:n ilmentymisen määrittämiseksi. Uusien hermosolujen lukumäärää verrattiin saman ryhmän terveeseen aivopuoliskoon ja kontrolliryhmään (n=6), joille oli injektoitu AAV:n sijaan suolaliuosta. Uusien hermosolujen määrä väheni paikallisesti AAV-injektion kohdealueella hiiren hippokampuksessa. Yllättäen yhteyttä fluoresenssin ja uusien hermosolujen vähenemisen välillä ei löytynyt. Tämä tutkielma tukee niitä harvoja tutkimuksia, jotka ovat raportoineet AAV:n haitoista aikuisiällä syntyneille hermosoluille. Koska AAV on laajalti käytössä geeniterapian sekä aivotutkimuksen työkaluna, on erittäin tärkeää huomioida nämä tulokset ja tehdä jatkotutkimuksia AAV:n mahdollisista haitoista eri solu- ja kudostyypeille, sekä selvittää näkyvätkö vaikutukset käytöksen tasolla esimerkiksi oppimisen yhteydessä.

TABLE OF CONTENTS

ABBREVIATIONS

AAV	adeno-associated virus
AHN	adult hippocampal neurogenesis
DCX	doublecortin
GECI	genetically encoded calcium indicator
GF	green fluorescence
GFP	green fluorescent protein
ITR	inverted terminal repeat
PBS	phosphate-buffered saline

1 INTRODUCTION

Memory allows individuals to reflect on their past experiences and knowledge, and subsequently use this information to cope with day-to-day life. Hippocampus is central to learning and memory, two processes that are widely intertwined. Particularly dentate gyrus, a part of the hippocampal formation, is commonly accepted as an important part of memory formation (reviewed in Aimone et al. 2014, Gonçalves et al. 2016). Disrupting the formation of new neurons impairs hippocampus-related functions of dentate gyrus (Clelland et al. 2009, Kesner et al. 2014, Nakashiba et al. 2012).

The formation of new neurons in adult brain is localized mainly in the subgranular zone of dentate gyrus, where dividing neural progenitor cells give rise to adult-born neurons. Through both morphological and physiological development, neural progenitor cells mature into adult-born dentate granule cells, which eventually integrate into hippocampal networks. This phenomenon is termed adult hippocampal neurogenesis (AHN) (reviewed in Aimone et al. 2014). A simplified process of AHN is illustrated in Figure 1. Another neurogenic niche of adult mammalian brain is in the subventricular zone in the lateral ventricles, from where new neurons travel to olfactory bulb to mature into local interneurons (reviewed in Alvarez-Buylla and García-Verdugo 2002). An ongoing debate surfaced during late 2010's about the existence of AHN in humans after Sorrells et al. (2018) had their article published in *Nature*. They concluded that only negligible number of new neurons are generated in human hippocampus after childhood. However, this finding has been contradicted by histological and functional studies (reviewed in Lucassen et al. 2020). Despite extensive studies focusing on AHN, the function of adult-born dentate granule cells is not fully clarified, and therefore research concerning neurogenesis is fundamental.

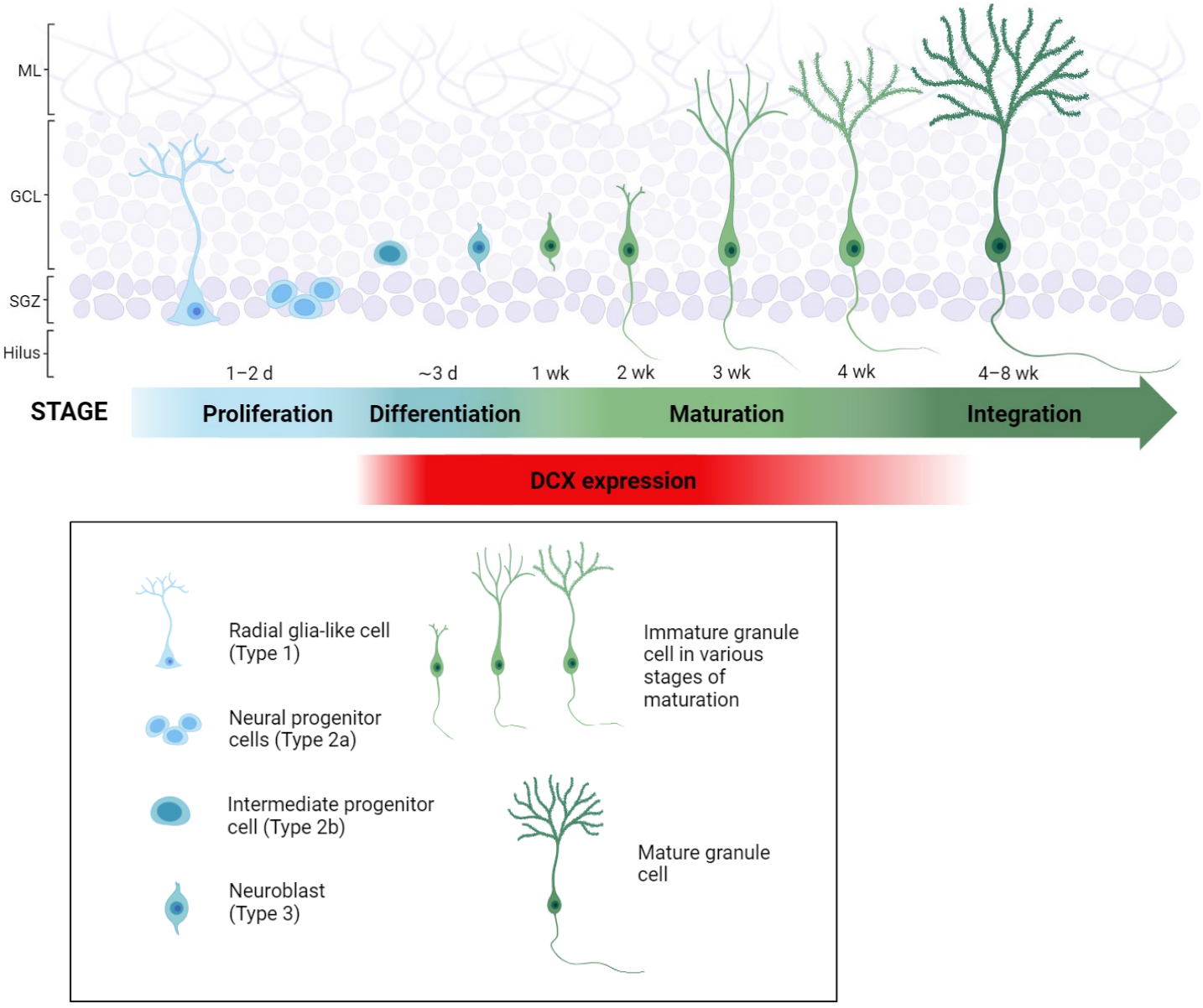

Figure 1. Simplified illustration of the process of adult hippocampal neurogenesis (AHN) in subgranular zone of hippocampal dentate gyrus. During AHN, radial glia-like cells (also known as type 1 cells) divide to produce neural progenitor cells (type 2a cells). Neural progenitor cells differentiate through an intermediate stage (type 2b cells) to neuroblasts (type 3 cells). Neuroblasts give rise to immature granule cells that go through both morphological and physiological maturation into mature granule cells, that will eventually integrate into hippocampal networks. Doublecortin (DCX) is expressed from differentiation of developing granule cells through the maturation of immature granule cells. Figure is drawn based on Aimone et al 2014, Brown et al 2003, Kempermann 2003, Kempermann et al. 2004 & 2015 and Ming and Song 2005 & 2011.

Multiple non-invasive methods, such as behavioral testing (reviewed in Savage and Ma 2014) and functional neuroimaging, including functional magnetic resonance imaging (fMRI) and positron emission tomography (PET) (reviewed in Cabeza and Nyberg 2000, Reber 2013) are used to study the processes of learning and memory but acquiring single cell resolution *in vivo* is not plausible with such techniques. In order to gain information about cellular level phenomena, like an activation of a cell, access to the cells is necessary. It can be achieved with genetically encoded calcium indicators (GECIs) when coupled with micro-optics. These GECIs are able to label a specific neuronal population, and combined with micro-optical tools they enable the imaging of deep brain regions and give access to large neuronal populations (Hayashi et al. 2017). Action potentials generate $Ca2^{+}$ influxes in the neuron terminals, and this phenomenon is put in use in GECIs, that are a fusion of fluorescent proteins and $Ca2^{+}$-binding proteins. For example, a fusion of circularly permuted enhanced green fluorescent protein (GFP) and calmodulin, coupled with calmodulin target peptide M13, gives rise to specific GECI family termed GCaMP. The imaging of neuronal activity with GCaMP relies on fluorescence increase which is caused by $Ca2^{+}$-dependent conformational change in the calmodulin-M13 complex. Upon binding $Ca2^{+}$, calmodulin interacts with M13, which restricts the access of water molecules to the chromophore. This causes deprotonation of the chromophore, which fluoresces brightly in this anionic form (Barnett et al. 2017). Engineering of the GCaMP family has resulted in GCaMP variants that can detect action potentials of single cells (Ahrens et al. 2013, Sofroniew et al. 2016). GCaMP variants are developed to yield e.g., better signal-no-noise ratios and fluorescence signals. GCaMP6 variants, used also in this study, were developed in 2013 and are divided to three subtypes based on their kinetics (Chen et al. 2013). These subtypes, GCaMP6s, GCaMP6m and GCaMP6f are named after the speed of the kinetics, with s standing for slow, m for medium and f for fast. The sensitivity of these GCaMP6 sensors is higher with slower kinetics and vice versa. GCaMP6s performs better at detecting single action potentials than the 6m and 6f sensors. Newer GCaMP variants have been since developed, with the newest (as of November 2023) being jGCaMP8 sensors with fastest kinetics and highest sensitivity to date (Zhang et al. 2023). In order to make cells of interest express fluorescent calcium indicator, the genes encoding given molecules have to be conveyed to the site. Adeno-associated viruses (AAVs) are among the most extensively used vectors for gene delivery (Wang et al. 2019).

AAVs belong to *Parvoviridae* family and are further classified to the *Dependoparvovirus* genus (Wu et al. 2006). *Dependeparvoviruses* are dependent on helper viruses, such as herpes simplex virus or adenovirus, to accomplish a successful viral life cycle. In absence of helper virus, AAV infection is latent and viral genes integrate in the host genome (Chen 2007) or remain in the cell as episomal forms (Deyle and Russell 2009, Bijlani et al. 2021). Recombinant AAVs rarely integrate into the host chromosomes, and the long-term expression is mainly a result of episomal concatemers constructed from intermediate forms of double-stranded DNA (Ferrari et al. 1996, Nakai et al. 2001, Wang et al. 2007). On

the rare occasions of AAV chromosomal integration, the designated integration site in human genome is the long arm of chromosome 19 at position 13.3qter, namely in *AAVS1* locus (Kotin et al. 1992, Dutheil et al. 2000).

Since AAVs do not replicate without helper viruses, and have low immunogenicity, they are generally regarded as safe, and have become intriguing genetic vectors (Naso et al. 2017). There are a handful of AAV-based gene therapy products in clinical use (e.g., U.S. Food and Drug Administration, 2017 and 2019) and multiple going through clinical trials for treating various diseases in virtually all types of tissues (Mingozzi and High 2011, Naso et al. 2017) including a myriad of treatments targeting the central nervous system (Hocquemiller et al. 2016, Ojala et al. 2014). For example, in 2019 U.S. Food and Drug Administration approved AAV9-based gene therapy (onasemnogene abeparvovec-xioi, brand name Zolgensma®) for treatment of spinal muscular atrophy (SMA) in children under the age of two. Patients suffering from SMA experience loss of voluntary muscle control, which stems from recessive inherited disorder in the survival motor neuron 1 (SMN1) gene. This disorder leads to depletion of certain nerve cells that are responsible for relaying information between spinal cord and skeletal muscle, resulting in motor impairment. Treatment with Zolgensma has been shown to improve motor function in children treated with it (for more extensive review, see Yang et al. 2023). However, in 2022 Novartis, the company marketing Zolgensma, confirmed that two patients had died following an acute liver failure after treatment with Zolgensma (Philippidis 2022), resulting in the risk/benefit profile of this gene therapy being called into question.

In recombinant AAVs (rAAVs), the genes to be transduced are packed between inverted terminal repeats (ITRs), that form the rim of viral genes (Wang et al. 2019), which are the sole part of wild type AAV present in recombinant AAVs. For clarity, in this thesis the abbreviation AAV is used when referring to recombinant AAVs.

In contrary to common belief of non-pathogenic nature of AAVs, some recent studies have found signs of harm induced by AAV in neural progenitor cells and immature dentate granule cells (Johnston et al. 2021) as well as other cell types (Hinderer et al. 2018, Hirsch et al. 2011). Johnston et al. (2021) reported that reduction of neural progenitor cells and immature dentate granule cells – the reduction of neurogenesis – induced by AAV transduction appears to be dose-dependent and happens with commonly used viral titers in experiments in mice dentate gyrus ($\geq 3 \times 10^{11}$ gc/ml, with injected volume of 1 µl). They studied the relationship between dose and time, but the longest follow-up time from injection to tissue collection was three months. In that study, cell death induced by AAV was not dependent on the used promoter, fluorescent protein or serotype among other procedures concerning AAV production.

Johnston and their colleagues (2021) also assessed the possible role of inflammation as the cause for reduction of adult-born neurons by microglia/macrophage-specific protein Iba1 (ionized calcium binding adaptor

molecule 1) and astrocyte specific GFAP labeling. Microglia are the main immune cells of the brain, whereas astrocytes support many functions, including structural and metabolic processes and inflammatory reactivity in response to injury (reviewed in Freeman and Rowitch 2013). The results that Johnston et al. (2021) obtained, do not support the idea, that inflammation resulted in reduction of neurogenesis, since Iba1 and GFAP levels rose 4 weeks after AAV-injection, whereas adult-born neurons were eliminated 48 hours post-injection. Instead, experiments denoted that ITRs mediated this decrease in neural progenitor cells and newly generated granule cells. This was studied by introducing ITR oligonucleotides to mouse neural progenitor cells *in vitro*. They observed a dose-dependent cell loss and arrest of proliferation of neural progenitor cells within hours to days. Given that AAVs rely on ITR-flanked genes, it is essential to further investigate the potential negative effects of AAV, especially when keeping in mind that AAVs are commonly used vectors in human gene therapy.

According to Kuzmin et al. (2021), already in early 2020's there were over 3,000 individuals treated with AAV vectors. Long-term follow-up research concerning AAV gene therapy durability and its persistent effect are sparse, but in the few conducted studies the transgene expression achieved with AAV vectors are shown to last for years (Xiao et al. 1996, Bijlani et al. 2021). In modern neuroscience, AAV-based research on learning and memory has gained ground ever since the realization that AAVs can be engineered to target cells in the central nervous system (for brief review, see Haggerty et al. 2019). These approaches also include calcium imaging via genetically encoded calcium indicators. Especially in *in vivo* models the different methods should not affect the quality or quantity of the data. Furthermore, given that AAVs are amongst the most popular vectors for delivering genetically encoded calcium indicators, the issue with AAV induced cell ablation raises concern.

This study was done to clarify the effect of AAV viral vector on neurogenesis by conducting immunohistochemical labeling and confocal microscopy from the brains of adult male CJ57BL/6J mice. Brain sections from mice, that received either AAV injection or control procedure 33 weeks earlier, were used to compare the effect of AAV transduction on neurogenesis. The volume of injection was 1 µl, and the used titer was 3.5×10^9 gc/ml, which is less than AAV titers commonly used for injections to the dentate gyrus (1.5×10^{12}–3.6×10^{13} gc/ml, injection volume 1 µl) (Johnston et al. 2021). Quantitative indicator of neurogenesis in this study was the number of doublecortin (DCX) -labeled newly born neuronal cells in the murine dentate gyrus. DCX is a microtubule-associated protein widely used as a marker for neurogenesis, especially for immature neurons (Couillard-Després et al. 2005, Spampanato et al. 2012), mainly neurons born within the last 12 days (Figure 1) (Rao and Shetty 2004, Kuipers et al. 2015). Maturing neurons have been observed to express DCX for up to a month after the generation of new neurons, albeit only in a fraction of the original DCX-expressing neuroblast population (Brown et al. 2003). DCX is

paramount for neuronal migration, and mutations in *Dcx* gene and DCX expression level have been shown to affect cell proliferation in addition to neuronal migration (Pramparo et al. 2010, Filipovic et al. 2012). The AAV9 vector used in this study carried calcium indicator GCaMP6s with neuron-specific CAMKII promoter. Even though CAMKII is quite often considered to be excitatory neuron-specific, Veres et al. (2023) have shown it to target other cell types, including inhibitory neuronal cells. However, they concluded that in hippocampus the percentage of the studied inhibitory cells that were targeted by CAMKII promoter was low, with only a fraction of inhibitory cells expressing CAMKII-driven transgene. So, it is reasonable to assume that in this study the transgene-expressing cells were excitatory apart from marginal exceptions.

In this study, the amount of GCaMP6s-derived green fluorescence (GF) in vicinity of the injection site was evaluated through confocal microscopy as an estimate of AAV transduction. Green fluorescent protein (GFP) is used as a gene reporter, and it can be used to quantitatively assess the amount of transgene expression in eukaryotic cells (see e.g., Anderson et al. 1996, Soboleski et al. 2005). GCaMPs are based on GFP, and GCaMP-derived GF has also been used as an estimate of transgene expression (see e.g., Dana et al. 2014). Control group was predisposed to AAV-lacking phosphate-buffered saline (PBS) injections and sham operations instead of viral vector and lens implantation. In light of recent research, it was hypothesized that AAV decreases neurogenesis in hippocampus. Also, the possible impact of microendoscopy when coupled with AAV injections in hippocampus was assessed by comparing the amount of neurogenesis in the two hemispheres of the brain. The hypothesis was that the healthy hemisphere would have more neurogenesis in comparison to the AAV-injected and lens implanted side.

2 MATERIALS AND METHODS

The invasive nature of this study requires animal models. For this purpose, 20 male C57BL/6JRcc/Hsd mice (Envigo, Netherlands) were housed in the animal facilities of University of Jyväskylä in groups of two to three animals per cage. Upon arrival at the age of four weeks, the animals were acclimatized to premises and handling for two weeks. Water and food were freely available, and the mice were maintained in 12 h/12 h light-dark cycles. Cardboard tubes were given to the mice as an enrichment. Animals were randomly assigned to experimental group that received AAV-injections and lens implantations (n=14) and control group, that received PBS injections and dummy implantations (n=6). From each individual, data from both hemispheres were treated individually, with the side without injection or implant serving as a contralateral inner control. Therefore, the formed groups were AAV implant, AAV control, PBS implant and PBS control. The general workflow of the study and the formed groups are depicted in Figure 2. This thesis is part of a larger research project titled "Dentate gyrus –

the gateway to memory?, and procedures on mice, i.e. animal maintenance, injections and implantations, were done by the research group. I cryosectioned the brains, immunolabeled the sections with DCX-antibody and performed the counting of adult-born neurons, as well as carried out fluorescence analyses.

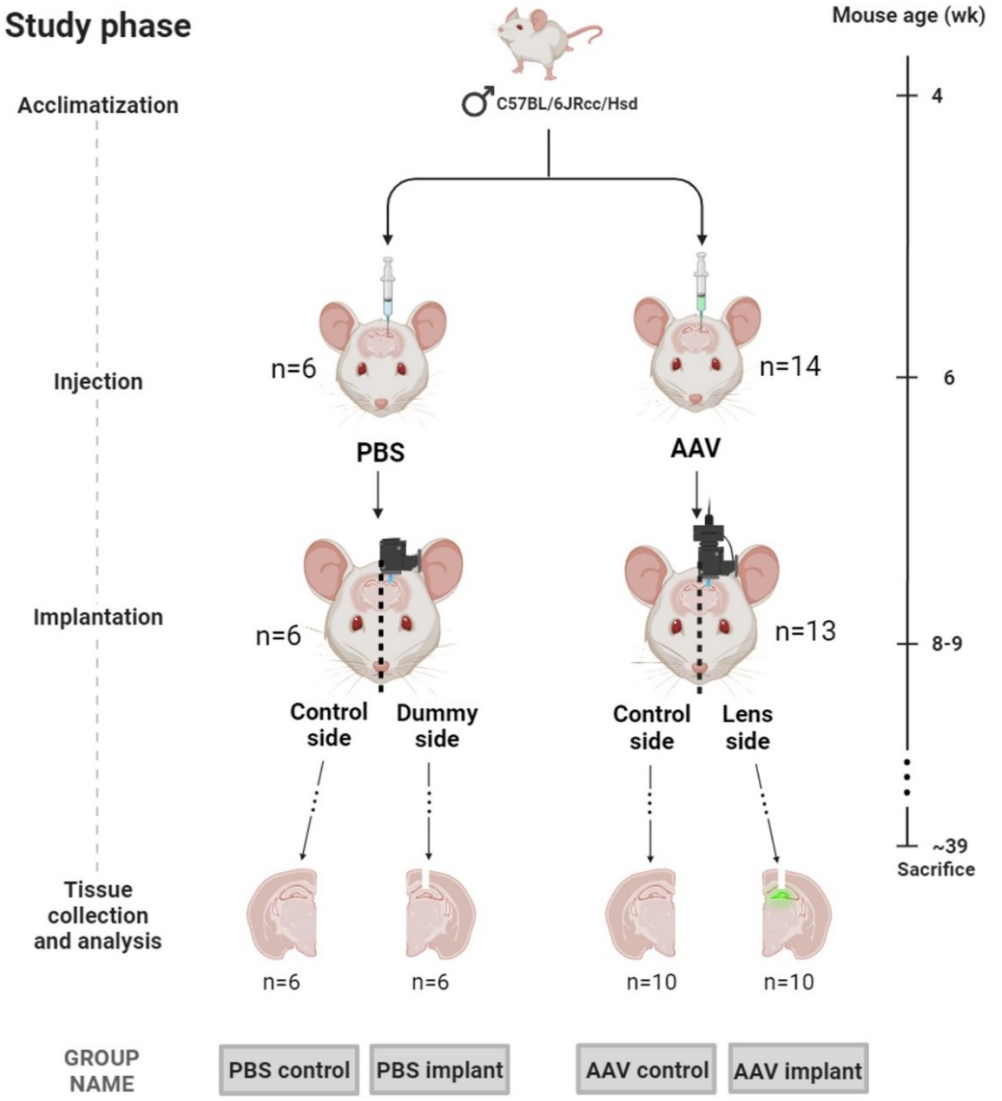

Figure 2. Flow chart of experiments on mice. Recombinant AAV9 vector was injected unilaterally to dentate gyri of adult male mice, to express calcium indicator GCaMP6s under CAMKII promoter. Control group received unilateral sterile PBS injections instead of AAV (control group designated hence PBS). For calcium imaging purposes, tiny glass lenses (microendoscopes) were implanted to injected hemispheres of AAV mice to image GCaMP6s expressing cells. Comparable cylindrical objects (dummies) were implanted to injected hemispheres of PBS mice. Contralateral hemispheres were consequently left intact. Therefore the formed groups were PBS control, PBS implant, AAV control

and AAV implant. In addition to calcium imaging, GCaMP6s-derived GF was used as a gene reporter for the amount of AAV transduction. During analysis, new-born adult neurons were immunolabeled with DCX-antibody to yield a numeric value to represent the amount of neurogenesis. Illustration depicts the injected and implanted hemisphere on the right by convention, although the unilateral injections and implantations were done to either hemisphere.

2.1 Ethical approval

Approval for all the procedures was given by Animal Experiment Board of Southern Finland (licence ESAVI/24666/2018) and conducted in accordance with directive 2010/63/EU of the European Parliament. Personnel working with animals had competence according to the FELASA guidelines.

2.2 Virus injection and lens implantation

Mice belonging to the AAV group (aged 6 weeks at the time, n=14) received AAV viral injections with a GCaMP6s gene under CAMKII promoter. Injections were done unilaterally to hippocampus to express GCaMP6s in the granule cells of hippocampal dentate gyrus. The expression of calcium-controlled fluorescence coupled with microendoscopy (implantation of small, permanent lens into the brain tissue) enables the imaging of neuronal activity in real-time. GCaMP6s also serves as a fluorescent marker for histology studies done with confocal microscopy. AAV.CamKII.GCaMP6s.WPRE.SV40 was a gift from James M. Wilson (Addgene viral prep #107790-AAV9; http://n2t.net/addgene:107790; RRID:Addgene_107790). AAV9 viral preparation was diluted to sterile PBS to reach a concentration of 3.5×10^9 gc/ml. During the injections, the mice were fixed to a manually operated stereotaxic frame. AAV solution was injected to four sites to ensure the success of injection. 250 nanoliters (100 nl/min) of AAV solution (3.5×10^9 gc/ml) was injected per injection site under isoflurane anesthesia. Therefore the total dose of AAV was 3.5×10^6 gc. Injection coordinates for the four injections were: i) anterior-posterior from bregma (A/P) -2.0, medial/lateral to midline (M/L) ± 1.4 mm and dorsal/ventral from dura (D/V) -2.3 mm, ii) A/P -2.0 mm, M/L ± 1.4 mm and D/V -2.1 mm, iii) A/P -2.0 mm, M/L ± 0.9 mm and D/V -2.3 mm, and iv) A/P -2.0 mm, M/L ± 0.9 mm and D/V -2.1 mm (Figure 3). The coordinates on Figure 3 are adapted from Paxinos and Franklin (2004), but because isoflurane anesthesia causes swelling of the brain, the illustrated injection sites do not align with theoretical stereotaxic coordinates, which are based on mouse brain under normal physiological conditions. However, the injection coordinates presented above were the ones used to adjust the stereotaxic frame. The animals received injections randomly to either left or right hemisphere of the brain. For control group (n=6) the procedure was done similarly, but instead of virus solution, sterile PBS was injected. After recovery period of approximately two to three weeks, chronic glass gradient index (GRIN) lens (Inscopix nVista™) for AAV mice or dummy (cylindrical object of similar

size) for control mice was implanted surgically under isoflurane anaesthesia to area showing GF or the site of control injection. By predisposing only one side of the brain to injections and lens/dummy implantation, the other side could be used as an internal reference to compare differences between hemispheres as well as between groups. One mouse had to be killed during the lens implantation for failure to express any signal. During the course of the study, three additional animals were found dead in their premises. All the dead animals belonged to the AAV group (final n=10).

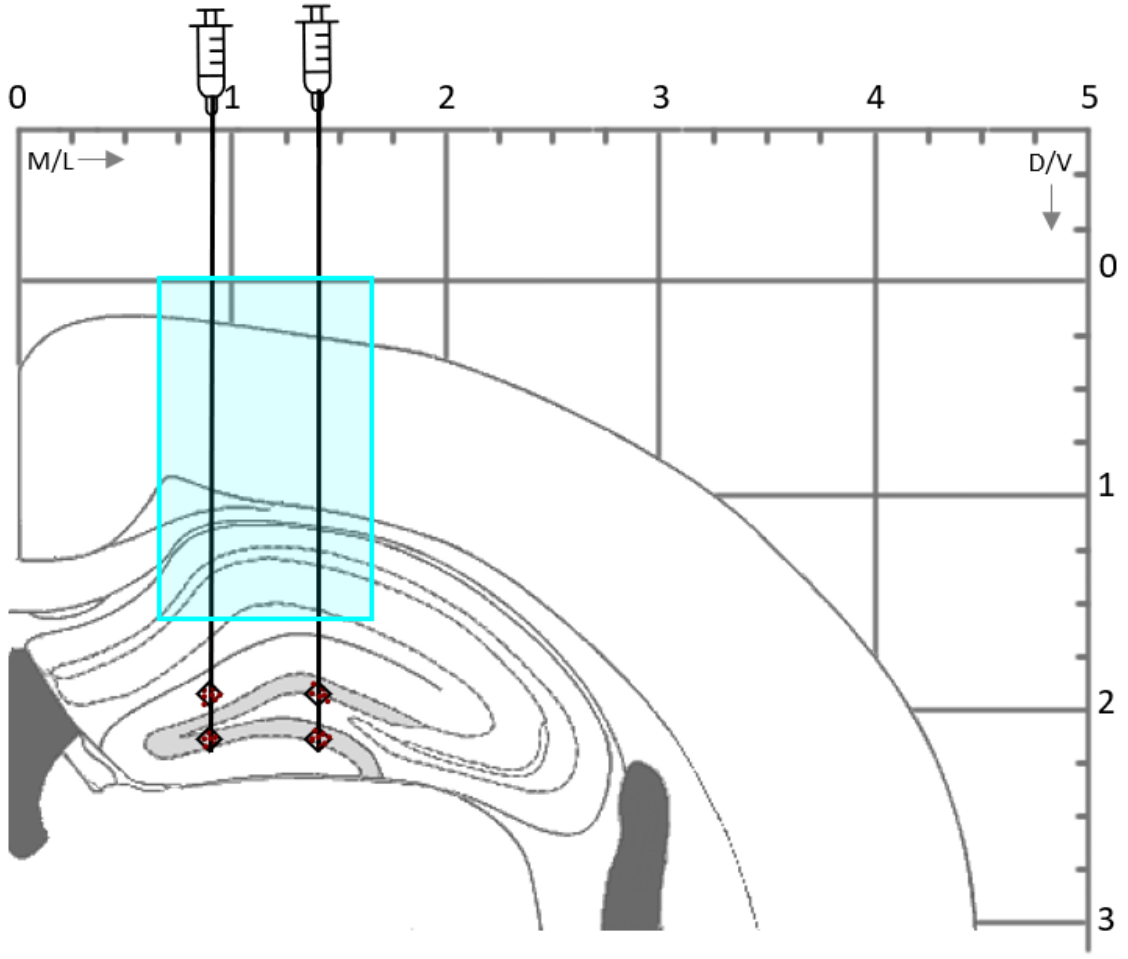

Figure 3. A schematic illustration of unilateral injection sites and implant placement. The implant was placed at approximately 300 µm distance from dentate gyrus, which is illustrated with light grey color. The distance was assessed by GF intensity recorded with Inscopix nVista™ from GCaMP6s expressing dentate granule cells. Quadrilaterals with red dots represent injection sites in dentate gyrus. Blue rectangle represents the implant placement. The coordinates of the illustration represent the medial/lateral to midline (M/L) direction on horizontal axis and dorsal/ventral from dura (D/V) on vertical axis. Figure is drawn based on stereotaxic coordinates from Paxinos and Franklin 2004.

2.3 Histology

At the time of the euthanasia, the animals were approximately 9 months old, and were considered to be young adults (see Dutta and Sengupta 2016). At this point, ca. 33 weeks had passed after AAV injections. The animals were killed with an overdose of sodium pentobarbital (*s.c.*), and the brains were perfusion fixed. Brains were washed with 0.9% NaCl-solution for four minutes (10 ml/min), after which they were perfused with fresh 4% paraformaldehyde solution (pH 7.4) for nine minutes (10 ml/min). Brains were post-fixed with 4% paraformaldehyde in PBS (pH 7.4) at +4˚C for maximum of 24 hours, after of which the solution was replaced with 0.1 M PBS (pH 7.4) and the brains were stored at +4˚C until sectioning.

At least 48 h before sectioning, brains were immersed in 30% sucrose to prevent freezing damage caused by dry ice and to preserve the brain morphology upon cryosectioning. To cut the brains, they were frozen with dry ice and sliced coronally into thin 40 µm sections using a sliding microtome (Leica SM2010 R, IL, USA). Every 12th section was collected to a tube containing cryoprotectant solution (18.75% w/v sucrose, 37.5% v/v ethylene glycol (VWR, #85512.290), 62.5% v/v 0.05 M phosphate buffer (PB), 0.025% w/v sodium azide (Sigma Aldrich, #S2002)). One tube per individual was randomly selected for further staining procedures.

2.4 Immunolabeling and confocal microscopy

To visualize adult-born neurons, sections were immunohistochemically stained according to a free-floating method described previously by Nokia et al. (2016) with modifications, because fluorescent labeling of target proteins was used. The used procedure is summarized in the next paragraph.

All the immunolabeling procedures were done under constant shaking at room temperature. The cryoprotectant solution was washed from the sections (three 10-minute washes) with 1X PBS (pH 7.4). Samples were blocked with normal goat serum (10% normal goat serum (Biowest, #S200H-500) in 1X PBS, supplemented with 0.3% Triton X-100 (Electran® Triton X-100, VWR, #437002A)) for 30 minutes. Primary antibody (polyclonal doublecortin produced in rabbit, Cell Signaling Technology, #4604), was diluted at 1:800 in 1X PBS supplemented with 1% normal goat serum and 0.3% Triton X-100, added to the samples, and incubated overnight. On the second day, the sections were washed with 1X PBS (three washes for 10 minutes each) and incubated 2 hours in secondary antibody solution (1:200 Alexa Fluor 546 goat anti-rabbit IgG, Invitrogen by Thermo Fisher Scientific, #A11035; diluted to 1X PBS supplemented with 1% normal goat serum and 0.3% Triton X-100). Washes were repeated as previously, and sections were mounted on microscope slides, allowed to dry and coverslipped. 4',6-diamidino-

2-phenylindole (DAPI) was incorporated into the mounting medium (VectaShield® HardSet™ Antifade mounting media with DAPI, Vector Laboratories, #H-1500) to visualize the nuclei in fluorescence microscopy.

The counting of the adult-born dentate granule cells and imaging the sections for analyzing the expression of GCaMP6s-derived GF intensity were done by fluorescence microscopy using Zeiss LSM 700 confocal microscope (Carl Zeiss Microscopy LLC, NY, USA). For imaging, DAPI, GFP and DCX were sequentially excited by illuminating the sample with 405 nm, 488 nm, and 555 nm lasers, respectively. For GFP, laser power was set to 0.4 mW, gain (voltage) to 463 V, and offset to 0. DAPI and DCX signals were not used for quantitative analyses, and therefore the adjustments of the laser scanning system were done so that it was possible to acquire visually qualifiable images. All the settings were kept identical between samples. Images were scanned unidirectionally with pixel dwell time of 1.58 µsec, and pinhole diameter of 11.5 µm (1.94 AU), 14.5 µm (2.14 AU), and 9.7 µm (1.37 AU) for DAPI, GFP and DCX, respectively. The emission filters were short pass 555 for GFP and long pass 490 for DCX. The location of the implant was assessed with the help of mouse brain atlas with stereotaxic coordinates (Paxinos and Franklin 2004). To measure GF, corresponding images were taken from hippocampi of both hemispheres with 10x magnification, and the lens/dummy was fitted to the obtained image, always with similar settings. Images of 2048 x 2048 pixels were taken using Zeiss Plan-Apochromat 10x (numeric aperture, NA=0.45) objective.

Three sections (à 40 µm) from each mouse were selected for counting of the DCX positive cells and imaging of the GF intensity, with one section from the position of the implant, one caudally, and one cranially to the implant. Due to the random sampling and implant dimensions, implant was occasionally visible in multiple sections. In such case, the section with implant diameter closest to one millimeter (i.e. midpoint of the implant) was chosen to represent the middle position of the implant. All cells located in the dentate gyrus with neuron-like structure were included in the counting of DCX positive cells. The average number of DCX positive cells in a section within the group was used as a marker of neurogenesis. The intensity of GF was measured with QuPath® (Bankhead et al. 2017) version 0.4.2. using the software intensity feature detector. The maximum and mean intensity values from images of three sections from each individual were averaged individually to obtain one value to represent each subject. In addition to mean value, maximum intensity was chosen to estimate the highest amount of fluorescence in the target area. The whole imaged area (2048 x 2048 pixels) was included in the intensity measurements in QuPath®.

2.5 Statistical analysis

Statistical analyses were done with IBM SPSS Statistics (version 29.0.0.0) software. To study the potential differences in mean values between the groups, a non-parametric Mann-Whitney U test was used since the distribution of the data violated the assumptions of parametric t-tests. For contralateral comparisons, i.e. within-subjects comparisons (PBS/AAV control vs. PBS/AAV implant), Wilcoxon signed-rank test was used. Spearman correlation was applied to test the correlation between the number of adult-born dentate granule cells and GCaMP6s-derived GF intensity, which was used as an estimate of AAV transduction.

3 RESULTS

To study the effect of recombinant AAV vector injection and chronically implanted lens on AHN, 3.5×10^6 gc of AAV9 vector carrying GCaMP6s calcium indicator was injected unilaterally to hippocampal dentate gyri of adult male mice (n = 10). Few weeks later, glass gradient index lenses were implanted on the side of the injection. Control group received PBS injections and sham implants of similar size to lens instead of experimental procedures. Unilateral operations allowed the contralateral hemisphere to stay intact and serve as an inner control. 33 weeks after the injections, the mice were euthanized and the number of adult-born neurons in the dentate gyrus was assessed from three coronal sections adjacent and at the location of the implant or from corresponding location of the intact hemisphere by immunolabeling with DCX antibody. Also, GCaMP6s-derived GF was measured as an estimate of the amount of AAV.

The unoperated hemisphere of AAV group (AAV control) did not differ in the amount of neurogenesis from either the PBS implant or PBS control group (Figure 4). The number of new neurons in the AAV implant group (mean = 8.30) was significantly lower than in the AAV control group (mean = 13.83) (Wilcoxon signed-rank test, $Z = -1.99$, $p = 0.047$). There were 40% less DCX positive cells in the hippocampus of the AAV implant group in comparison to contralateral side of the AAV injection (Figure 5).

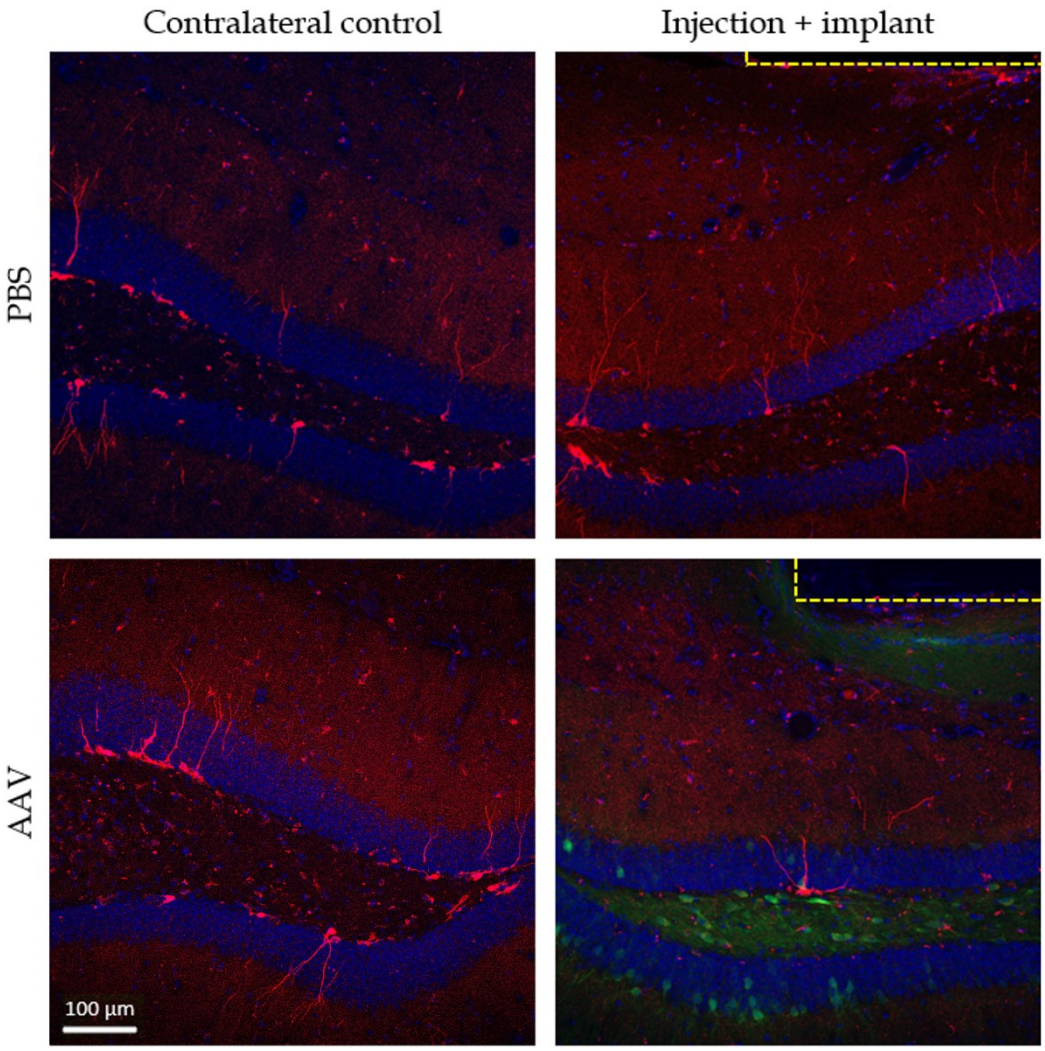

Figure 4. Representative confocal microscopy images from coronal sections of mouse brain. Dentate gyri of adult male mice were unilaterally injected with recombinant AAV9 vector to express calcium indicator GCaMP6s under CAMKII promoter. Control group received unilateral sterile PBS injections instead of AAV. Contralateral hemispheres served as controls for both the AAV and PBS injections. 33 weeks after injections, adult hippocampal neurogenesis was visualized by immunolabeling with doublecortin (DCX)-antibody. Images show the cell nuclei in the granule cell layer of the dentate gyrus labeled with DAPI (blue), GCAMP6s-derived green fluorescence (GF) (green) and DCX positive cells (red). The images used for quantification were obtained with Zeiss LSM700 confocal microscope with 10x magnification, whereas these images were taken with 20x magnification to allow better visualization. Lens position is indicated with yellow dashed line. Images are otherwise original, but the brightness and contrast were enhanced for visual purposes. The scalebar is shown in the lower left panel and is the same in all images.

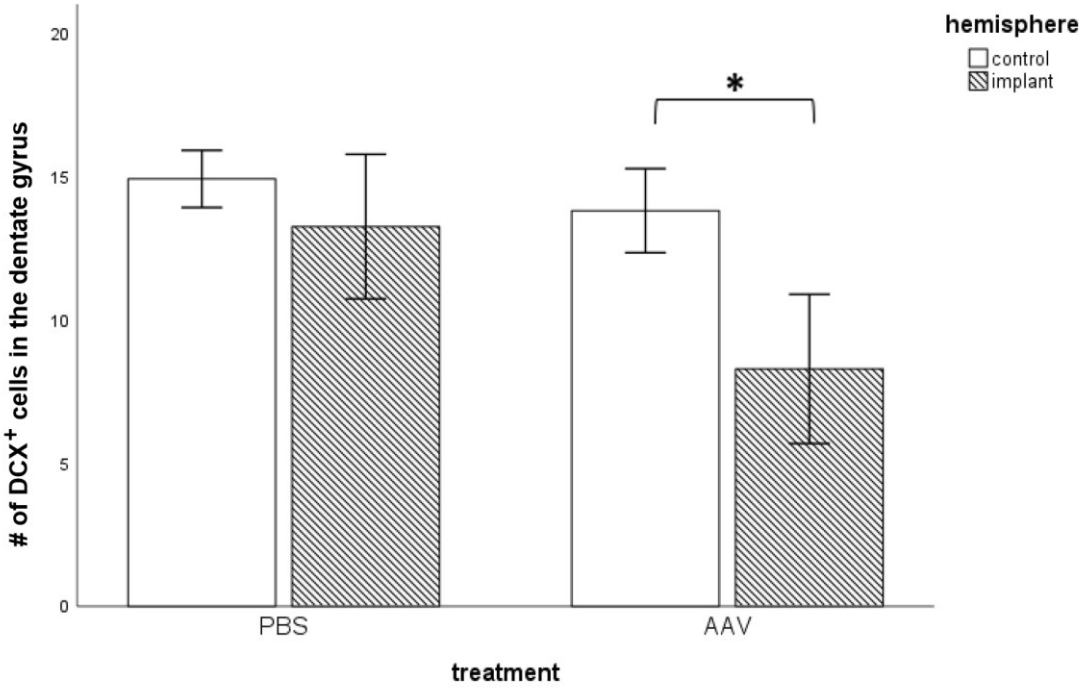

Figure 5. To measure neurogenesis, newly generated neurons were immunolabeled with doublecortin-antibody (DCX) in the brains of AAV-injected (n=10) and PBS-treated control (n=6) mice. The number of DCX expressing cells (mean +/- SE) in the granule cell layer of the dorsal hippocampal dentate gyrus was counted from three representative sections per animal and their average value was used as an indicator of neurogenesis in each animal. For the statistical comparisons Wilcoxon signed-rank test was used. * $p < 0.05$.

The number of adult-born neurons between the two hemispheres of PBS group correlated positively ($r = 0.611$, $p = 0.007$). On the contrary, in the AAV group there was no correlation in the number of new neurons between the two hemispheres ($r = 0.332$, $p = 0.073$). In other words, there were equal number of new neurons in the hemispheres of PBS group (Figure 5). However, GF intensity and the number of DCX positive cells did not correlate in any of the groups (Spearman correlation; PBS control: $r = 0.338$, $p = 0.512$, PBS implant: $r = 0.092$, $p = 0.321$, AAV control: $r = 0.195$, $p = 0.590$ and AAV implant: $r = 0.212$, $p = 0.556$). Thus, GF intensity, i.e., GCaMP6s expression, did not explain the amount of neurogenesis in any of the groups. Both the maximum and average intensity of GF, measured from AAV control side were less than fifth of that on AAV implant side, whereas only minuscule fluorescence was detected in the PBS group (Figure 6).

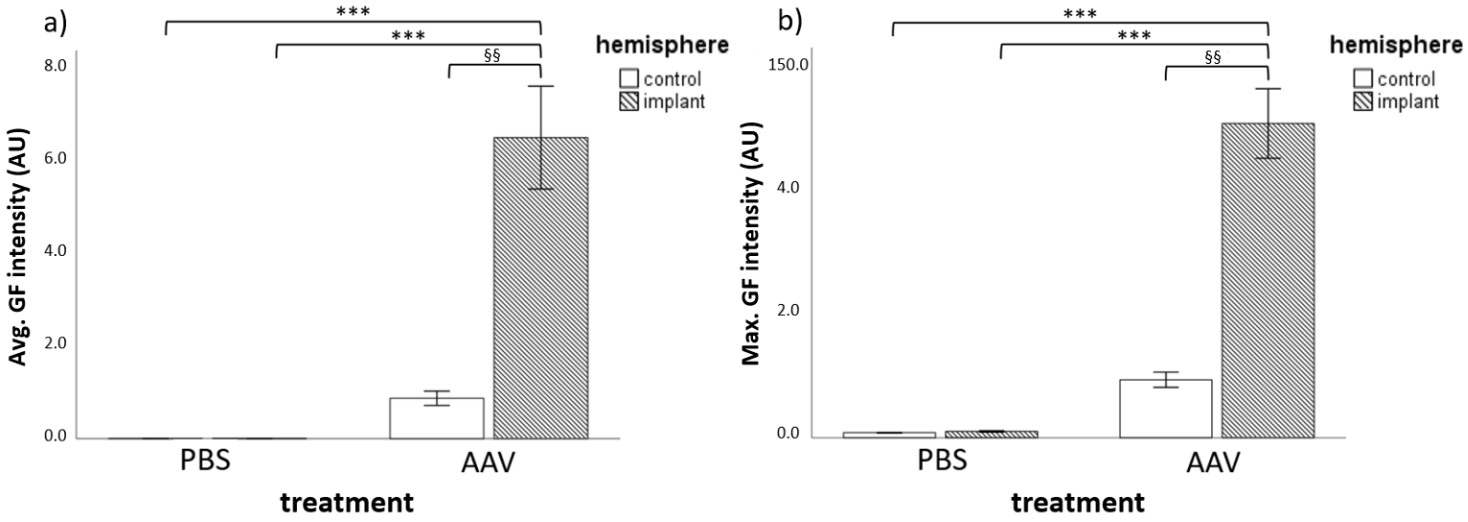

Figure 6. The intensity of GF (arbitrary units, AU), i.e., GCaMP6s expression was measured with QuPath® software's intensity feature detector from imaged sections of hippocampi from AAV-injected (n=10) and PBS-treated (n=6) mice. The implant was similarly fitted to all images, and the corresponding location was imaged from contralateral hemisphere. The intensity was defined as a) average intensity (mean +/- SE), and b) maximum intensity (mean +/- SE). Statistical comparisons between groups were done with Mann-Whitney *U* test, *** $p \leq 0.001$, and within-subjects comparisons were done with Wilcoxon signed-rank test, §§ $p \leq 0.01$.

4 DISCUSSION

Recent research has challenged the long-thought safety of AAV as a gene therapy vector as it was found that AAV viral vectors cause cell death among adult-born neurons (e.g., Johnston 2021). In this thesis, this was studied further by comparing the number of adult-born neurons in the mouse hippocampus between two groups, one of which received unilateral AAV injections (n=10) and implantations of calcium imaging-permitting chronic glass lenses to the hippocampus, and the other served as the control group (n=6) exposed to sterile PBS injections and dummy implantations. The unilateral injections permitted using the intact hemispheres as internal controls. The AAV construct encoded calcium indicator GCaMP6s, carrying GFP gene under neuron-specific CAMKII promoter, which enables *in vivo* neuronal imaging when coupled with micro-optical tools. The main finding of the study was that in the group subjected to AAV injections and implantation of microendoscopic lens, the neurogenesis was significantly reduced in contrast to controls, as was originally hypothesized. The harmful effect of AAV to new neurons expressing DCX was localized on the brain hemisphere subjected to AAV injections, and the contralateral hemisphere did

not differ in the amount of neurogenesis from the sham control. In their study, Johnston et al. (2021) found that the loss of adult-born dentate granule cells during intermediate progenitor cell stages (see Figure 1, cell types 2a, 2b and 3), as well as during immature stages (during DCX expression) after AAV injections did not recover during follow-up time. Intermediate progenitor cells were quantified up to 4 weeks post-injection, whereas immature cells for 3 months. My results indicate that recovery of immature adult-born dentate granule cells is not apparent even after 33 weeks (ca. 7.5 months). In unaffected state, the maturing dentate granule cells in hippocampus are replaced by progenitor cells, but by virtue of the results of Johnston et al. (2021), showing the loss of intermediate progenitor cells, this replacement has not likely happened. That supports the idea that the AAV-induced neuron loss can be sustained for longer periods of time, which was observed also here.

In more detail, this thesis demonstrates that injecting 3.5×10^6 gc of AAV9 vector carrying GCaMP6s into dentate gyrus of mouse reduces adult hippocampal neurogenesis (Figure 5). Unexpectedly, the number of adult-born neurons did not correlate with the GCaMP6s expression. Under the assumption that the expression of AAV would lead to the reduction of neurogenesis, and that the amount of GCaMP6s-derived GF would reflect AAV-driven transgene expression, it is counterintuitive to not find correlation between these two. It may be that the microendoscopy had an impact on the neurogenesis instead of the viral vector, but this ought to have been registered also in the sham operation group. On the other hand, the intensity of GF on histological preparations can possibly have been subjected to decrease of fluorescence intensity due to prolonged preservation of the samples. This could have affected the measured intensity, and therefore diminished the correlation. However, comparisons of immunofluorescently labeled sections from different time points did not support this explanation. To control this, I measured GF intensity from randomly chosen sections approximately two months after the first fluorescence measurement and compared the intensities from different timepoints, and there was no decrease in the GF. Another alternative is that the AAV expression and fluorescence do not coincide, i.e., the fluorescence can not be used as a direct measure of AAV expression, or that moderate variations in GF intensity, reflecting GCaMP6s expression, do not influence AHN. Regardless of the reason for this lack of correlation, it is a subject that deserves further research.

Here, I analyzed both average and maximum intensity values, even though usually, when GFP is used as a gene reporter, it is done with average values (see e.g., Soboleski et al. 2005). To examine a scenario, in which multiple cells show high GF intensity, maximum value was used as an alternative unit of measure. Overexpression of proteins, also reported on GFP, is associated with oxidative stress on the cell (Ganini et al. 2017), cellular deficits and even cell death (Mori et al. 2020, Detrait et al. 2002). The overexpression of GFP, introduced by a reporter gene, is shown to result in cell death also in neuronal populations (see e.g., Detrait et al. 2002). GCaMP calcium indicators are based on GFP, and there is

evidence that GCaMP6 expression, especially during development (mice younger than 7 weeks of age), can result in epileptiform activity (Steinmetz et al. 2017). Additionally, GCaMP overexpression has been shown to induce cytotoxic effects and disrupt calcium homeostasis in mouse brain (Tian et al. 2009). These aberrancies are detected in cells, that express GCaMP in the cell nuclei, whereas GCaMP expression in cytosol does not lead to these negative impacts. In this study, visual assessment showed multiple cells overexpressing GCaMP6s, which was marked by nuclear filling of the cells (Figure 4, lower right panel) (Chen et al. 2013, Resendez et al. 2016). High levels of GCaMP expression, e.g., by high titers or long-term expression, have been shown to disrupt calcium dynamics and signalling via channel perturbations and even lead to apoptosis. Therefore, to get an optimal GCaMP expression without the downsides of overexpression, it is advisable to perform the experiments within three to eight weeks post-injection. Longer time windows have been shown to increase the side effects of GCaMP expression (Resendez et al. 2016, Yang et al. 2018). In this study, the mice were perfused ca. 33 weeks post-injection, which could have resulted in higher expression levels than optimal. The nuclear filling seen in many GCaMP-expressing cells substantiates this hypothesis. The slow turn-over rate of neurons has likely enabled the long-term expression of GCaMP in the target cells, increasing the probability of side effect appearance. Also, the work mechanism of GCaMP, notably calmodulin binding intracellular $Ca2^+$ to produce a fluorescent signal, might lead to buffering of $Ca2^+$ by GCaMP (McMahon and Jackson 2018). In an experimental setup, where intracellular $Ca2^+$ is monitored as an indicator of e.g., neuronal signaling during learning, $Ca2^+$ buffering by the research tool, let alone plausible emergence of side effects is unwanted. However, potential disruptive or deleterious effect of GCaMP expression itself could not be assessed by the experimental design and would require additional studies.

No GF was detected in the PBS groups in addition to minuscule fluorescence, which most likely stems from autofluorescence. This is supported by the observation, that low levels of autofluorescence were detected from brain tissue, that did not receive GCaMP6s-coding AAV injections, or were part of the PBS groups. Although neurogenesis was reduced in AAV implant group, no observable difference in well-being of the animals was seen, and the animals grew comparably between groups (data not shown). The sham implant (dummy), coupled with PBS injections did not create an impact on AHN, so the operations themselves did not affect the amount of neurogenesis.

Possible limitation of this study is the use of only male mice, even though it has been noted that sex and sex-related hormones have an impact on neurogenesis (Duarte-Guterman et al. 2015). However, the research group is conducting a similar study with female mice, and the results can be widely combined to yield data that can be generalized to include both sexes. Also, no group lacking all procedures was included, and the absence of negative control may have influenced the interpretation of the results. However, it is not likely that the sham control group would have rendered a falsely significant result,

since this would have been the case only if the sham control group would have gained benefit from the treatment.

Johnston et al. (2021) demonstrated that the AAV-induced reduction of neurogenesis correlates with the activity of dentate gyrus, and even titers that leave AHN intact influence the networks and their activity. In research, where adult-born dentate granule cells or their contribution to hippocampal functions is assessed, the changes in dentate gyrus activity can create a bias in the achieved results. The ablation of neurogenesis has been linked to poorer performance on multiple experimental tasks related to learning and memory on rodents (reviewed in Deng et al. 2010). According to Lensu et al. (2021), unilateral irradiation of rat brain reduces AHN and leads to impaired spatial memory, which underlines the importance of carefully choosing which vector to use for transgene delivery and acquiring certainty that the vector does not interfere with neuronal populations. When AAV is used for instance for delivery of calcium indicator to dentate gyrus, the possible ablation of adult-born neurons can influence the performance of the animals on cognitive tests, and therefore produce biased data. However, no difference in behavior between groups was found in another study on the same mice regarding the effect of the conducted operations on behavior and AHN. The mice were subjected to open field task, and hippocampus-dependent learning tasks before and after the injections, as well as after the implantations and their performance was not affected by the operations (S.-M. Lehtonen, unpublished). Also, it has been known for a while that neurogenesis is reduced with age, proved also in mice (Bondolfi et al. 2003, Kempermann et al. 1998). Even though this might have been a contributing factor, it does not explain the differences between groups of the same age. Other environmental factors, such as stress are shown to mediate AHN (reviewed in Warner-Schmidt and Duman 2006, Balu and Lucki 2009). However, these factors were controlled in the experimental design of this study by exposing all the mice to same treatments regardless of their designated group.

As a way to overcome the issue of AAV-induced cell loss, Johnston and their colleagues (2021) proposed using retrograde AAV transgene delivery, first introduced by Tervo et al. (2016). In this approach, projection neurons deliver the transgenes to the location of interest. Johnston et al. (2021) had used this method to successfully label cells in dentate gyrus without inducing reduction of AHN. However, the impact of this labeling on the target tissue itself was not assessed, and hence does not provide fail-safe way to tackle the questionability of AAV. In conclusion, this study underlines the importance of re-evaluating the safety of AAV-based gene therapies, particularly when keeping in mind that there are already clinically used AAV-based gene therapy products. These results should be taken into account when considering general guidelines of gene therapy applications and to stay cautious when deeming an approach as of lacking side effects. Also, when conducting research concerning dentate granule cells, the use of AAVs should be carefully evaluated. Also, the dose and delivery strategy of the viral vector, as well as experiment duration should be carefully selected to diminish AAV-mediated harm.

ACKNOWLEDGEMENTS

I would like to thank my supervisors for support during the thesis, Sanna Lensu for continuous help with immunolabeling, imaging of the fluorescent samples, statistical analyses and writing process and Jari Ylänne for comments on the written thesis. Also, I would like to thank all the staff that took part in the study, from people taking care of the animals to the ones giving advice when needed and everyone in between. This thesis was part of a larger research project titled "Dentate gyrus – the gateway to memory?" funded by Academy of Finland.

Jyväskylä November 12, 2023
Veera Puumalainen

REFERENCES

Ahrens M.B., Orger M.B., Robson D.N., Li J.M. & Keller P.J. 2013. Whole-brain functional imaging at cellular resolution using light-sheet microscopy. *Nat. Methods* 10(5): 413-420.

Aimone J.B., Li Y., Lee S.W., Clemenson G.D., Deng W. & Gage F.H. 2014. Regulation and function of adult neurogenesis: From genes to cognition. *Physiol. rev.* 94(4): 991-1026.

Alvarez-Buylla A. & García-Verdugo J.M. 2002. Neurogenesis in adult subventricular zone. *J. Neurosci.* 22(3): 629-634.

Anderson M.T., Tjioe I.M., Lorincz M.C. Parks D.R., Herzenberg L.A., Nolan G.P. & Herzenberg L.A. 1996. Simultaneous fluorescence-activated cell sorter analysis of two distinct transcriptional elements within a single cell suing engineered green fluorescent proteins. *Proc. Natl. Acad. Sci.* 93(16): 8508-8511.

Balu D.T. & Lucki I. 2009. Adult hippocampal neurogenesis: regulation, functional implications, and contribution to disease pathology. *Neurosci. Biobehav. Rev.* 2009 33(3): 232-252.

Bankhead P., Loughrey M.B., Fernández J.A., Dombrowski Y., McArt D.G., Dunne P.D., McQuaid S., Gray R.T., Murray L.J., Coleman H.G., James J.A., Salto-Tellez M. & Hamilton P.W. 2017. QuPath: open source software for digital pathology image analysis. *Sci. Rep.* 7: 16878. doi:10.1038/s41598-017-17204-5.

Barnett L.M., Hughes T.E. & Drobizhev M. 2017. Deciphering the molecular mechanism responsible for GCaMP6m's Ca2+-dependent change in fluorescence. *PLOS ONE* 12(2): e0170934. doi:10.1371/journal.pone.0170934.

Bijlani S., Pang K.M., Sivanandam V., Singh A. & Chatterjee S. 2021. The role of recombinant AAV in precise genome editing. *Front. Genome Ed.* 3: 799722. doi:10.3389/fgeed.2021.799722.

Bondolfi L., Ermini F., Long J.M., Ingram D.K., & Jucker M. 2003. Impact of age and caloric restriction on neurogenesis in the dentate gyrus of C57BL/6 mice. *Neurobiol. Aging* 25(3): 333–340.

Brown J.P., Couillard-Després S., Cooper-Kuhn C.M., Winkler J., Aigner L. & Kuhn G. 2003. Transient expression of doublecortin during adult neurogenesis. *J. Comp. Neurol.* 467: 1-10.

Cabeza R. & Nyberg L. 2000. Neural bases of learning and memory: functional neuroimaging evidence. *Curr. Opin. Neurol.* 13(4): 415–421.

Chen H. 2007. Comparative Observation of the Recombinant Adeno-Associated Virus 2 Using Transmission Electron Microscopy and Atomic Force Microscopy. *Microsc. Microanal.* 13: 384–389.

Chen T., Wardill T.J., Sun Y., Pulver S.R., Renninger S.L., Baohan A., Schreiter E.R., Kerr R.A., Orger M.B., Jayaraman V., Looger L.L., Svoboda K., & Kim

D.S. 2013. Ultrasensitive fluorescent proteins for imaging neuronal activity. *Nature* 499: 295-300.

Clelland C.D., Choi M., Clemenson G.D., Fragniere A., Tyers P., Jessberger S., Saksida L.M., Barker R.A., Gage F.H. & Bussey T.J. 2009. A functional role for adult hippocampal neurogenesis in spatial pattern separation. *Science* 325(5937): 210-213.

Couillard-Després S., Winner B., Schaubeck S., Aigner R., Vroemen M., Weidner N., Bogdahn U., Winkler J., Kuhn H. & Aigner L. 2005. Doublecortin expression levels in adult brain reflect neurogenesis. *Eur. J. Neurosci*. 21: 1-14.

Dana H., Chen T.-W., Hu A., Shields B.C., Guo C., Looger L.L., Kim D.S. & Svoboda K. 2014. *Thy1*-GCaMP6 transgenic mice for neuronal population imaging *in vivo*. *PLoS ONE* 9(9): e108697. doi:10.1371/journal.pone.0108697.

Deng W., Aimone J.B. & Gage F.H. 2010. New neurons and new memories: how does adult hippocampal neurogenesis affect learning and memory? *Nat. Rev. Neurosci.* 11(5): 339-350.

Detrait E.R., Bowers W.J., Halterman M.W., Giuliano R.E., Bennice L., Federoff H.J. & Richfield, E.K. 2002. Reporter Gene Transfer Induces Apoptosis in Primary Cortical Neurons. *Mol. Ther.* 5(6), 723–730.

Deyle D.R. & Russell D.W. 2009. Adeno-associated virus vector integration. *Curr. Opin. Mol. Ther.* 11(4): 442-447.

Duarte-Guterman P., Yagi S., Chow C. & Galea L.A. 2015. Hippocampal learning, memory, and neurogenesis: Effects of sex and estrogens across the lifespan in adults. *Horm. Behav.* 74: 37-52.

Dutheil N., Shi F., Dupressoir T. & Linden M. 2000. Adeno-associated virus site-specifically integrates into a muscle-specific DNA region. *PNAS* 97(9): 4862-4866.

Dutta S. & Sengupta P. 2016. Men and mice: relating their ages. *Life Sci.* 152: 244-248.

Ferrari F.K., Samulski T., Shenk T. & Samulski R.J. 1996. Second-strand synthesis is a rate-limiting step for efficient transduction by recombinant adeno-associated virus vectors. *J. Virol.* 70(5): 3227-3234.

Filipovic R., Kumar S.S., Fiondella C. & Loturco J. 2012. Increasing doublecortin expression promotes migration of human embryonic stem cell-derived neurons. *Stem Cells* 30(9): 1852-1862.

Freeman M.C. & Rowitch D.H. 2013. Evolving concepts of gliogenesis: a look way back and ahead to the next 25 years. *Neuron* 80(3): 613-623.

Ganini D., Leinisch F., Kumar A., Jiang J., Tokar E.J., Malone C.C., Petrovich R.M. & Mason R.P. 2017. Fluorescent proteins such as eGFP lead to catalytic oxidative stress in cells. *Redox Biol.* 12: 462-468.

Gonçalves J.T., Schafer S.T. & Gage F.H. 2016. Adult neurogenesis in the hippocampus: from stem cells to behavior. *Cell* 167(4): 897-914.

Haggerty D.L., Grecco G.G., Reeves K.C. & Atwood B. 2019. Adeno-associated viral vectors in neuroscience research. *Mol. Ther. Methods Clin. Dev.* 17: 69-82.

Hayashi Y., Yawata S., Funabiki K. & Hikida T. 2017. *In vivo* calcium imaging from dentate granule cells with wide-field fluorescence microscopy. *PLoS ONE* 12(7): e0180452. doi:10.1371/journal.pone.0180452.

Hinderer C., Katz N., Buza E.L., Dyer C., Goode T., Bell P., Richman L.K. & Wilson J.M. 2018. Severe Toxicity in Nonhuman Primates and Piglets Following High-Dose Intravenous Administration of an Adeno-Associated Virus Vector Expressing Human SMN. *Hum. Gene Ther*. 29(3): 285-298.

Hirsch M.L., Fagan B.M., Dumitru R., Bower J.J., Yadav S., Porteus M.H., Pevny L.H. & Samulski R.J. 2011. Viral single-strand DNA induces p53- dependent apoptosis in human embryonic stem cells. *PLoS ONE* 6(11): e27520. doi:10.1371/journal.pone.0027520.

Hocquemiller M., Giersch L. Audrain M, Parker S. & Cartier N. 2016. Adeno-associated virus-based gene therapy for CNS diseases. *Hum. Gene Ther.* 27(7): 478-496.

Johnston S., Parylak S.L., Kim S., Mac N., Lim C., Gallina I., Bloyd C., Newberry A., Saavedra C.D., Novak O., Gonçalves J.T., Gage F.H. & Shtrahman M. 2021. AAV ablates neurogenesis in the adult murine hippocampus. *eLife* 10: e59291. doi:10.7554/eLife.59291.

Kempermann G., Kuhn H.G., & Gage F.H. 1998. Experience-induced neurogenesis in the senescent dentate gyrus. *J. Neurosci.* 18(9): 3206–3212.

Kempermann G. 2003. Early determination and long-term persistence of adult-generated new neurons in the hippocampus of mice. *Development* 130(2): 391–399.

Kempermann G., Jessberger S., Steiner B., & Kronenberg G. 2004. Milestones of neuronal development in the adult hippocampus. *Trends Neurosci.* 27(8), 447–452.

Kempermann G., Song H. & Gage F.H. 2015. Neurogenesis in the adult hippocampus. *Cold Spring Harb. Perspect. Biol.* 7(9):a018812. doi: 10.1101/cshperspect.a018812.

Kesner R.P., Hui X., Sommer T., Wright C., Barrera V.R. & Fanselow M.S. 2014. Postnatal neurogenesis is supporting remote memory and spatial metric processing. *Hippocampus* 24: 1663-1671.

Kotin R.M., Linden R.M. & Berns K.I. 1992. Characterization of a preferred site on human chromosome 19q for integration of adeno-associated virus DNA by non-homologous recombination. *EMBO J.* 11(13): 5071-5078.

Kuipers S.D., Schroeder J.E. & Trentani A. 2015. Changes in hippocampal neurogenesis throughout early development. *Neurobiol. Aging* 36(1): 365-379.

Kuzmin D.A., Shutova M.V., Johnston N.R., Smith O.P., Fedorin V.V., Kukushkin Y.S., van der Loo J.C.M. & Johnstone E.C. 2021. The clinical landscape for AAV gene therapies. *Nat. Rev. Drug Discov.* 20: 173-174.

Lensu S., Waselius T., Mäkinen E., Kettunen H., Virtanen A., Tiirola M., Penttonen M., Pekkala S. & Nokia M.S. 2020. Irradiation of the head reduces adult hippocampal neurogenesis and impairs spatial memory, but leaves overall health intact in rats. *Eur. J. Neurosci.* 53(6): 1885-1904.

Lucassen P.J., Fitzsimons C.P., Salta E. & Maletic-Savatic M. 2020. Adult neurogenesis, human after all (again): classic, optimized, and future approaches. *Behav. Brain Res.* 381: 112458. doi:.1016/j.bbr.2019.112458.

McMahon S.M. & Jackson M.B. 2018. An inconvenient truth: calcium sensors are calcium buffers. *Trends Neurosci.* 41(12): 880-884.

Ming G. & Song H. 2005. Adult neurogenesis in the mammalian central nervous system. *Annu. Rev. Neurosci.* 28: 223-250.

Ming G. & Song H. 2011. Adult neurogenesis in the mammalian brain: significant answers and significant questions. *Neuron* 70(4): 687–702.

Mingozzi F. & High K.A. 2011. Therapeutic in vivo gene transfer for genetic disease using AAV: progress and challenges. *Nat. Rev. Genet.* 12(5): 341-355.

Mori Y., Yoshida Y., Satoh A. & Moriya H. 2020. Development of an experimental method of systemically estimating protein expression limits in HEK293 cells. *Sci. Rep.* 10:4789. doi:10.1038/s41598-020-61646-3.

Nakai H., Yant S.R., Storm T.A., Fuess S., Meuse L. & Kay M.A. 2001. Extrachromosomal recombinant adeno-associated virus vector genomes are primarily responsible for stable liver transduction in vivo. *J. Virol.* 75(15): 6969-6976.

Nakashiba T., Cushman J.D., Pelkey K.A., Renaudineau S., Buhl D.L., McHugh T.J., Rodriguez Barrera V., Chittajallu R., Iwamoto K.S., McBain C.J., Fanselow M.S. & Tonegawa S. 2012. Young dentate granule cells mediate pattern separation, whereas old granule cells facilitate pattern completion. *Cell* 149(1): 188-201.

Naso M.F., Tomkovics B., Perry W.L. & Strohl W.R. 2017. Adeno-associated virus (AAV) as a vector for gene therapy. *BioDrugs* 31: 317–334.

Nokia M.S., Lensu S., Ahtiainen J.P., Johansson P.P., Koch L.G., Britton S.L. & Kainulainen H. 2016. Physical exercise increases adult hippocampal neurogenesis in male rats provided it is aerobic and sustained. *J. Physiol.* 594: 1855-1873.

Ojala D.S., Amara D.P. & Schaffer D.V. 2014. Adeno-associated virus vectors and neurological gene therapy. *Neuroscientist* 21(1): 84-98.

Paxinos G. & Franklin K.B.J. 2004. *The mouse brain in stereotaxic coordinates,* 2nd ed. Academic Press, San Diego.

Philippidis A. 2022. Novartis confirms deaths of two patients treated with gene therapy zolgensma. *Hum. Gene Ther.* 33(17-18): 842-844.

Pramparo T., Youn Y.H., Yingling J., Hirotsune S. & Wynshaw-Boris A. 2010. Novel embryonic neuronal migration and proliferation defects in *Dcx* mutant mice are exacerbated by *Lis1* reduction. *J. Neurosci.* 30(8): 3002-3012.

Rao M.S. & Shetty A.K. 2004. Efficacy of doublecortin as a marker to analyse the absolute number and dendritic growth of newly generated neurons in the adult dentate gyrus. *Eur. J. Neurosci.* 19(2): 234-246.

Reber P.J. 2013. The neural basis of implicit learning and memory: a review of neuropsychological and neuroimaging research. *Neuropsychologia* 51(10): 2026–2042.

Resendez S.L:, Jennings J.H., Ung R.L., Namboodiri V.M.K., Zhou Z.C., Otis J.M., Nomura H., McHenry J.A., Kosyk O. & Stuber G.D. 2016. Visualization of cortical, subcortical and deep brain neural circuit dynamics during naturalistic mammalian behavior with head-mounted microscopes and chronically implanted lenses. *Nat. Protoc.* 11(3): 566-597.

Savage S. & Ma D. 2014. III. Animal behaviour testing: memory. *Br. J. Anaesth.* 113(1): 6–9.

Soboleski M.R., Oaks J. & Halford W.P. 2005. Green fluorescent protein is a quantitative reporter of gene expression in individual eukaryotic cells. *FASEB J.* 19(3): 440-442.

Sofroniew N.J., Flickinger D., King J. & Svoboda K. 2016. A large field of view two-photon mesoscope with subcellular resolution for in vivo imaging. *eLife* 5: e14472. doi:10.7554/eLife.14472.

Sorrells S.F., Paredes M.F., Cebrian-Silla A., Sandoval K., Qi D., Kelley K.W., James D., Mayer S., Chang J., Auguste K.I., Chang E.F., Gutierrez A.J., Kriegstein A.R., Mathern G.W., Oldham M.C., Huang E.J., Garcia-Verdugo J.M., Yang Z. & Alvarez-Buylla A. 2018. Human hippocampal neurogenesis drops sharply in children to undetectable levels in adults. *Nature* 555: 377-381.

Spampanato J., Sullivan R.K., Turpin F.R., Bartlett P.F. & Sah P. 2012. Properties of doublecortin-expressing neurons in the adult mouse dentate gyrus. *PLoS ONE* 7(9): e41029. doi:10.1371/journal.pone.0041029.

Tervo D.G.R., Hwang B.-Y., Viswanathan S., Gaj T., Lavzin M., Ritola K.D., Lindo S., Michael S., Kuleshova E., Ojala D., Huang C.-C., Gerfen C.R., Schiller J., Dudman J.T., Hantman A.W., Looger L.L., Schaffer D.V. & Karpova, A.Y. 2016. A designer AAV variant permits efficient retrograde access to projection neurons. *Neuron,* 92(2): 372–382.

U.S. Food and Drug Administration, Center for Drug Evaluation and Research. Luxturna BLA 125610 approval letter. December 19, 2017. Retrieved April 5, 2022, from https://www.fda.gov/media/109487/download.

U.S. Food and Drug Administration, Center for Drug Evaluation and Research. Zolgensma BLA 125694 approval letter. May 24, 2019. Retrieved April %, 2022, from https://www.fda.gov/media/126130/download.

Wang D., Tai P.W.L. & Gao G. 2019. Adeno-associated virus vector as a platform for gene therapy delivery *Nat. Rev. Drug Discov*. 18(5): 358–378.

Wang J., Xie J., Lu H., Chen L., Hauck B., Samulski R.J. & Xiao W. 2007. Existence of transient functional double-stranded DNA intermediates during recombinant AAV transduction. *Proc. Natl. Acad. Sci. USA.* 104(32): 13104-13109.

Warner-Schmidt J.L. & Duman R.S. 2006. Hippocampal neurogenesis: opposing effects of stress and antidepressant treatment. *Hippocampus* 16(3): 239–249.

Wu Z., Asokan A. & Samulski J. 2006. Adeno-associated virus serotypes: vector toolkit for human gene therapy. *Mol. Ther.* 14(3): 316-327.

Xiao X., Li J. & Samulski R.J. 1996. Efficient long-term gene transfer into muscle tissue of immunocompetent mice by adeno-associated virus vector. *J. Virol.* 70(11): 8098-8108.

Yang D., Ruan Y. & Chen Y. 2023. Safety and efficacy of gene therapy with onasemnogene abeparvovec in the treatment of spinal muscular atrophy: a systematic review and meta-analysis. *J. Paediatr. Child Health* 59(3): 431-438.

Yang X., Liu N., He Y., Liu Y., Ge L., Zou L., Song S., Xiong W. & Liu X. 2018. Improved calcium sensor GCaMP-X overcomes the calcium channel perturbations induced by the calmodulin in GCaMP. *Nat. Comm.* 9: 1504. doi: 10.1038/s41467-018-03719-6.

Zhang Y., Rózsa M., Liang Y., Bushey D., Wei Z., Zheng J., Reep D., Broussard G.J., Tsang A., Tsegaye G., Narayan S., Obara C.J., Lim J.X., Patel R., Zhang R., Ahrens M.B., Turner G.C., Wang S.S., Korff W.L., Schreiter E.R., Svoboda K., Hasseman J.P., Kolb I., Looger L.L. 2023. Fast and sensitive GCaMP calcium indicators for imaging neural populations. *Nature* 615(7954): 884-891.